5-2020

The Long Time Behavior of the Predator-Prey Model with Holling Type III

Regen S. McGee

The University of Southern Mississippi

The Long Time Behavior of the Predator-Prey Model with Holling Type III

by

Regen McGee

A Thesis
Submitted to the Honors College of
The University of Southern Mississippi
in Partial Fulfillment
of the Requirements for the Degree of
Bachelor of Science
in the School of Mathematics and Natural Sciences

May 2020

Approved by

Zhifu Xie, Ph.D., Thesis Adviser
Professor of Mathematics

Bernd Schroeder, Ph.D., Director
School of Mathematics and Natural Sciences

Ellen Weinauer, Ph.D., Dean
Honors College

Abstract

In this paper, the classical Lotka-Volterra model is expanded based on functional response of Holling type III to analyze a dynamical predator-prey relationship with hunting cooperation (α) and the Allee effect among predators. The stability of equilibrium solutions was first analyzed by deriving a Jacobian matrix from partial derivatives of our model. Newly derived eigenvalues are then used to determine the stability. The viability of the model is then demonstrated by using MATLAB. The numerical results show a clear Allee effect and a variety of possible phenomena related to stability when carrying capacity (κ) is varied. Two different types of bifurcations are then observed from our numerical results.

Key Words: Lotka-Volterra model, Predator-Prey Interaction, Hunting cooperation, Allee effect, eigenvalues, Bifurcation, Equilibrium Coexistence, Stability Analysis

Acknowledgments

I would like to sincerely thank my research partners Jakolbia Shipmon and Jairus Simmons for their assistance. I am very grateful for the opportunity that Dr. Zhifu Xie, Dr. Huiqing Zhu, and The University of Southern Mississippi's Mathematics Department provided me with. Without the support and patience of Dr. Xie, this would not have been as fluid of a process. I have known Dr. Xie for four years, and his love for teaching and mathematics are contagious. I would also like to thank the Wright W. and Annie Rea Cross Endowment Scholarship and the Mathematics Association of America NREUP Program funded by the NSF Grant DMS-1652506. Without these funds, none of this research would have been possible.

Table of Contents

List of Illustrations

Chapter 1

Literature Review

Mathematical models have shown value in the examination of population dynamics with regards to food chain analysis with complicated spatiotemporal dynamics. An important factor which many modern models have adopted is the presence of cooperative behavior in populations. Cooperative behavior within species has been shown to be an important phenomenon affecting population demographics and thereby exhibiting an effect on results to their respective predator-prey models [1]. These behaviors may stimulate an Allee effect (correlation between population density and growth rate) and are thought by some to be vitally important and at the forefront of emerging conservation and management strategies [1, 2]. Courchamp et al. defined Allee effects as being either strong (having a critical population to sustain proliferation) or weak (no critical population needed) [1]. They also provided a distinction for component Allee effects (increase in population correlates to increase in individual fitness) and demographic Allee effects (increase in overall individual fitness correlates to increase in population).

Zhou and coworkers were early pioneers in modifying classical predator-prey models to include the impacts of Allee effects on population stability [3]. They started with the classic Lotka-Voterra model and accounted for three different Allee effects. Stability was assessed via phase-plane analysis. With regards to cooperative behavior in species, well-established modes of cooperation in prey (cooperative reproduction, foraging capacity, etc.) have led to pervasive modeling of populations exhibiting Allee effects in prey [4, 5, 6]. For instance, Wang and coworkers modeled a reaction-diffusive predator-prey system with a strong Allee effect in prey and using a Holling type-II functional response.

Because of the large focus on Allee effects in prey, a particularly interesting opportunity to model predators exists. One cooperative behavior of predators, hunting cooperation, exists among many predator populations, especially ones of critical concern [7]. Berec demonstrated the use of mathematical models on analyzing population dynamics of this specific cooperative among predators [8]. The study explored how predator-prey dynamics set by a Holling type-II functional responses, are modified by foraging facilitation in predators (i.e. cooperative hunting). Under the knowledge that foraging facilitation is a component Allee effect, Berec determined whether its presence invoked strong demographic Allee effects and whether it had an overall effect on predator-prey dynamics.

Spawning from this work, Alves and Hilker went backwards in complexity, and showed the use of the model on a more simplistic level [7]. This study utilizes a classic predator-prey model known as the Lotka-Volterra model and adds hunting cooperation in a similar manner which Berec did. The Lotka-Volterra model is represented as:

$$\begin{pmatrix} \frac{dN}{dt} = rN(1-\frac{N}{K}) - \phi(N,P)P, \\ \frac{dP}{dt} = e\phi(N,P)P - mP, \end{pmatrix} \tag{1.1}$$

Results from the study show relationships between increased predator survival rates and increased hunting cooperation as well as decreased survival rates with over-cooperation. However, the study also acknowledges that the model is a special case; it assumes a linear functional response. This means oscillations in the model only result from the presence of hunting cooperation, not its absence. It is also operating under the assumption that the predator attack rate increases with predator density and that predators benefit from their cooperative hunting behavior. Its results also reflect that of a very basic predator-prey model. Although an important conclusion of the study shows a more intricate model equation using a Holling type-III functional response can be obtained.

The use of different Holling-type functional responses in predator-prey models have proven to give better understanding of various population dynamics [9, 10, 11]. For this reason, we hypothesize the use of a hunting cooperation model with Holling type-III functional response will yield added diversity for modeling population dynamics with hunting cooperation of predators as a consideration. These results will be useful for special-concern species requiring critical analysis for their populations.

Chapter 2

Methodology

The relationship between predator and prey has been a driving force upon ecosystems throughout evolution. The coexistence of the two entities creates a system of give and take or checks and balances. The presence of either the predator or prey should not create an unstable system, but instead should allow the predator and prey to live harmoniously in a stable environment. With cooperative behavior of predators, a positive relationship between the per capita growth rate and population density, also known as Allee effect, results [5]. Previously, Allee effects have been primarily studied in prey, but Allee effects in predators can be attributed to size-selective predation, mate-limitation, or foraging facilitation among predators[5].

It can induce a positive relationship between the per capita growth rate and population density, which is called a demographic Allee effect (Stephens et al., 1999; Courchamp et al., 2008). This effect can potentially lead to population extinction, which has recently seen renewed interest in both theoretical and empirical studies of biological conservation in endangered or exploited ecosystems

The classical Lotka-Volterra model with logistic growth of the prey and hunting cooperation is written as:

$$\begin{pmatrix} \frac{dN}{dt} = rN(1-\frac{N}{K}) - \phi(N,P)P, \\ \frac{dP}{dt} = e\phi(N,P)P - mP, \end{pmatrix} \tag{2.1}$$

where N and P are prey and predator densities respectively, r is the per capita intrinsic growth rate of prey, K is a carrying capacity of prey, e is the conversion efficiency and m is the per capita mortality rate of predators. Here all parameters are positive, and the function $\phi(N,P)$ is the functional response of predator on prey.

For our case, we have the Holling type III functional response

$$\phi(N,P) = \frac{\rho(P)N^2}{1+H_1\rho(P)N^2}, \tag{2.2}$$

where H_1 is greater than zero, and the attack or encounter rate is $\rho(P) = \lambda + aP$.

The Holling type III functional response is found in predator-prey relationships where predators increase their search activity proportionally to prey density. Birds are popularly known for behaving this way with prey densities such as fish. The predator's behavior in Holling type III is unlike the predator's behavior with Holling type II functional response. With Holling type II, predator search activity will stay constant no matter the prey density. Predation can vary within Holling type IV functional response as well, but the predator's search rate is hindered rather than increased as prey densities increase rapidly.

In the following, to simplify our model, we will consider a standard non-dimensionalized version of (2.1) with the functional response (2.2). Introducing the dimensionless variables and parameters

$$\begin{aligned} n = \sqrt{\frac{e\lambda}{m}}N; p = \sqrt{\frac{\lambda}{em}}P; \tau = mt, \\ \sigma = \frac{r}{m}; \kappa = \sqrt{\frac{e\lambda}{m}}K; \alpha = \frac{a}{\lambda}\sqrt{\frac{em}{\lambda}}; h_2 = H_2\frac{m}{e}; \end{aligned} \tag{2.3}$$

with the addition of model (2.2), model (2.1) becomes

$$\begin{pmatrix} \frac{dn}{d\tau} = n[\sigma(1-\frac{n}{k}) - \frac{(1+\alpha p)np}{1+h_2(1+\alpha p)n^2}], \\ \frac{dp}{d\tau} = p[\frac{(1+\alpha p)n^2}{1+h_2(1+\alpha p)n^2} - 1], \end{pmatrix} \tag{2.4}$$

where σ represents the relative growth rate, κ (carrying capacity) contains dimensional K, e, and m in a non-dimension parameter, and hunting cooperation is represented as α.

To understand the dynamical behavior of the predator and prey over the long time period, we conduct linear stability analysis of the equilibrium solutions (or called fixed points, or steady states) of the model (2.4). An equilibrium solution of the model (2.4) is a constant solution (n, p) which satisfies the corresponding algebraic equation:

$$\begin{pmatrix} n[\sigma(1-\frac{n}{k}) - \frac{(1+\alpha p)np}{1+h_2(1+\alpha p)n^2}] = 0, \\ p[\frac{(1+\alpha p)n^2}{1+h_2(1+\alpha p)n^2} - 1] = 0. \end{pmatrix} \tag{2.5}$$

It is easy to find the boundary equilibrium solutions: $(0,0)$ and $(\kappa,0)$. To find the coexistence equilibrium solutions, we need to solve a third order polynomial equation. Instead of deriving a complex expression, we conduct a numerical search for coexistence equilibrium solutions for certain well-chosen parameters in Chapter 4.

Once equilibrium solutions are found, we conduct linear stability analysis by computing the

Jacobian matrix and its eigenvalues. The long time behavior of the evolution of the predator and the prey may be predicted by the results of linear stability analysis. In the following chapters, we carry out the discovery of equilibrium solutions and stability analysis. We pay more attention on how the parameters affect the number of equilibrium solutions, their stability, and possible Allee effect.

Chapter 3

Stability Analysis of Boundary Equilibrium Solutions

We follow the standard procedures to conduct linear stability analysis for a general two-dimensional system:

$$\begin{pmatrix} \dfrac{dx}{dt} = f(x,y), \\ \dfrac{dy}{dt} = g(x,y). \end{pmatrix} \tag{3.1}$$

Suppose that $(\bar{x},\bar{y})$ is an equilibrium solution, that is $f(\bar{x},\bar{y}) = 0$ and $g(\bar{x},\bar{y}) = 0$. The Jacobian matrix of the ODE system (3.1) at the equilibrium solution $(\bar{x},\bar{y})$ is defined as

$$J = \begin{pmatrix} J_{11} & J_{12} \\ J_{21} & J_{22} \end{pmatrix} = \begin{pmatrix} \frac{\partial f}{\partial x}(\bar{x},\bar{y}) & \frac{\partial f}{\partial y}(\bar{x},\bar{y}) \\ \frac{\partial g}{\partial x}(\bar{x},\bar{y}) & \frac{\partial g}{\partial y}(\bar{x},\bar{y}) \end{pmatrix}. \tag{3.2}$$

The linear stability of the equilibrium solution $(\bar{x},\bar{y})$ is determined by the eigenvalues of the matrix, as follows:

- If the eigenvalues of the Jacobian matrix all have real parts less than zero, then the equilibrium solution is stable.
- If at least one of the eigenvalues of the Jacobian matrix has real part greater than zero, then the equilibrium solution is unstable.
- Otherwise there is no conclusion (then we have a borderline case between stability and instability; such cases require an investigation of the nonlinear stability analysis, and this requires more sophisticated mathematical machinery discussed in advanced courses on ordinary differential equations).

Thus, the procedure to determine the linear stability of an equilibrium solution $(\bar{x},\bar{y})$ in the ODE system (3.1) is as follows:

1. Compute all partial derivatives of the right-hand side of the original system of differential equations, and construct the Jacobian matrix.
2. Evaluate the Jacobian matrix at the steady state.
3. Compute eigenvalues.

4. Conclude stability or instability based on the real parts of the eigenvalues.

In this section, we derive two variants of the Jacobian matrix J for the model that is tuned to effectively aid in the stability analysis of each boundary solution. We then present both sufficient and necessary conditions for stability of each equilibrium solution for our system. In general, the Jacobian matrix J for the model (2.4) about an equilibrium solution (n, p) is

$$J = \begin{pmatrix} \sigma - \frac{2n\sigma}{\kappa} - \frac{(2np(1+ap)}{(1+h_2n^2+h_2\alpha pn^2)^2} & \frac{-n(n\alpha^2p^2h_1+2\alpha pnh_1+h_1n+2p\alpha-1)}{(1+h_1n+h_1\alpha pn)^2} \\ \frac{2np(1+ap)}{(1+h_2n^2+h_2\alpha pn^2)^2} & \frac{(n^2+2\alpha pn^2)(1+h_2n^2+\alpha pn^2h_2)-(pn^2+\alpha p^2n^2)(\alpha n^2h_2)}{(1+h_2n^2+h_2\alpha pn^2)^2} - 1 \end{pmatrix}. \tag{3.3}$$

The characteristic polynomial for the Jacobian matrix J can be given as $f(\lambda) = \lambda^2 - Trace(J)\lambda + Det(J)$. Then

$$\lambda = \frac{Trace \pm \sqrt{Trace^2 - 4Det(J)}}{2} \tag{3.4}$$

are two eigenvalues of the Jacobian matrix J. To guarantee stability of a solution, we must ensure that our eigenvalue is negative for real eigenvalues or ensure that the real part of the complex eigenvalue is negative for complex eigenvalues. This leads us to the following necessary and sufficient conditions to guarantee stability.

- $Trace(J) = J_{11} + J_{22}$ must be less than zero.
- $Det(J) = J_{11}J_{22} - J_{12}J_{21}$ must be greater than zero.

Theorem 1. (Linear Stability of Boundary Solutions). The boundary equilibrium solution $(0,0)$ is always unstable, and the stability of $(k,0)$ is dependent upon the value of $-1 + (-h_2+1)K^2$. When $-1+(-h_2+1)K^2 < 0$, the equilibrium solution $(k,0)$ is stable, and when $-1+(-h_2+1)K^2 > 0$, it is unstable.

Proof. In order to analyze the stability for $(0,0)$, we substitute $n = 0$ and $p = 0$ in our general form of the Jacobian matrix (3.3). As a result, our Jacobian now simplifies to the following matrix:

$$J = \begin{pmatrix} \sigma & 0 \\ 0 & -1 \end{pmatrix}$$

Since we know that our sufficient and necessary criteria for stability, where $trace(J) < 0$ and $det(J) > 0$, we impose those conditions in our J. This gives us the following equations:

$$Trace = (-1) + \sigma, Det = (-1)(\sigma).$$

From algebraic analysis, it is evident that $(0,0)$ is always unstable because once these values are used to compute eigenvalues, we are able to determine that: $\lambda_1 = -1 < 0$, $\lambda_2 = \sigma > 0$ or that $Det = -1\sigma < 0$ for all $\sigma > 0$. Therefore, $(0,0)$ is always an unstable equilibrium.

Again, we compute the Jacobian for $(n,p) = (\kappa,0)$, which simplifies to the following matrix:

$$J = \begin{pmatrix} -\sigma & \frac{-\kappa^2}{1+h_2\kappa^2} \\ 0 & \frac{-1+(-h_2+1)\kappa^2}{(1+h_2\kappa^2)} \end{pmatrix}.$$

Now, with $trace(J) < 0$ and $det(J) > 0$, we are able to derive the following equations to determine stability:

$$Trace = \frac{-1+(-h_2+1)\kappa^2}{1+h_2\kappa^2} - \sigma, \quad Det = \frac{\sigma+(-h_2+1)(-\kappa^2\sigma)}{1+h_2\kappa^2}.$$

Since we know that our sufficient and necessary criteria for stability, where $trace(J) < 0$ and $det(J) > 0$, we impose those conditions in our J. This gives us the following inequalities:

$$\begin{pmatrix} \frac{-1+(-h_2+1)\kappa^2}{1+h_2\kappa^2} - \sigma < 0 \\ \frac{\sigma+(-h_2+1)(-\kappa^2\sigma)}{1+h_2\kappa^2} > 0 \end{pmatrix} \tag{3.5}$$

From the above equations we can say, if $(-1+(-h_2+1)\kappa^2) < 0$ we get the $trace < 0$ and the $Det > 0$ resulting in the equilibrium $(\kappa,0)$ being stable. On the other hand, if $(-1+(-h_2+1)\kappa^2) > 0$, we have the $Det < 0$, which means the equilibrium $(\kappa,0)$ is unstable.

□

The linear stability of an equilibrium solution can tell the long time behavior of a solution starting from a point near the equilibrium solution. Assume the system parameters satisfy $(-1+(-h_2+1)\kappa^2) < 0$. If the prey and predator start from (n^*,p^*) which is near to the equilibrium $(\kappa,0)$, the predator approaches extinction and prey achieves its maximum capacity after a long time (see Figure 4.4 (a)). Coexistence of predator and prey does not occur.

Chapter 4

Numerical Analysis for Equilibrium Solutions of Coexistence

As described in Chapter 3, we shall first find the coexistence equilibrium solutions. Then we compute the corresponding Jacobian Matrix and its eigenvalues to determine linear stability. On the other hand, when we graph the solution curves starting near an equilibrium solution, we are able to numerically determine the stability of the equilibrium solution on phase planes and check the Allee effect. Nullclines provide information about the number of coexistence equilibria. The first nullcline, which is the nontrivial predator and prey (total) is derived from the addition of two equations (2.5). The second nullcline, the nontrivial predator nullcline, is found by directly solving for p in the second equation in (2.5). The results are:

$$\begin{pmatrix} p = n\sigma - \dfrac{n^2\sigma}{\kappa}, \\ p = \dfrac{n^2 - 1 - h_2 n^2}{-\sigma n^2 + \sigma n^2 h_2}. \end{pmatrix} \tag{4.1}$$

In the first quadrant of the np-plane, an intersection of two curves of (4.1) gives an equilibrium solution. As we tried to solve for the nontrivial equilibrium solutions by eliminating p in (4.1), the resulting fourth order polynomial equation is hard to solve. We turn to numerical computations for some well-chosen parameters $\kappa, \sigma, h_2, \alpha$ to illustrate the rich dynamical properties of our model (2.4).

Example 1 (number of coexistence equilibrium varying κ): Given $\sigma = 20, h_2 = 0.9, \alpha = 0.1$. The number of coexistence equilibrium solutions changes as the carrying capacity, κ, is varied. Figure 4.1 shows the nullclines in the np-plane where κ varies from 2 to 5. The possible number of coexistence equilibrium solutions are zero, one, and two.

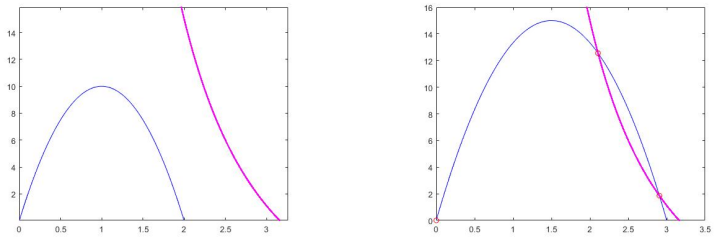

(a) $\kappa = 2$ (b) $\kappa = 3$

(c) $\kappa = 4$ (d) $\kappa = 5$

Figure 4.1: The number of intersections of nullclines are zero for $\kappa = 2$, two for $\kappa = 3$, one for $\kappa = 4$ and 5.

Example 2 (Numerical Observation): Given $\kappa = 3, \sigma = 20, h_2 = 0.9, \alpha = 0.1$ besides boundary equilibrium solutions $(0,0), (\kappa,0)$, we have two coexistence equilibrium solutions (see Figure 4.1 (b)): $(2.106, 12.555)$ a stable node, and $(2.904, 1.857)$ an unstable saddle point (see Figure 4.2).

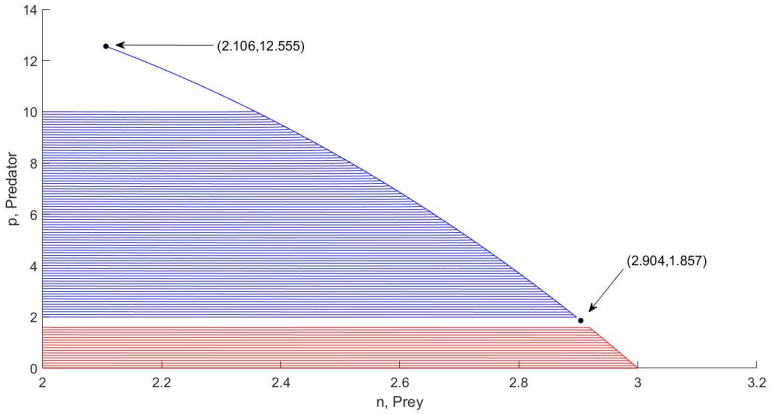

Figure 4.2: Phase portraits illustrate that the equilibrium solution $(2.106, 12.555)$ is stable, and $(2.904, 1.857)$ is unstable.

In order to derive the results in Example 2, we first substitute the parameters $\kappa = 3, \sigma = 20, h_2 = 0.9, \alpha = 0.1$ into equations (4.1). Using MATLAB, it is easy to obtain two coexistence equilibrium solutions $(2.106, 12.555)$ and $(2.904, 1.857)$. Considering the equilibrium $(2.106, 12.555)$, we determine the stability by computing the corresponding

Jacobian matrix (3.3):

$$J = \begin{pmatrix} 0.0557 & 1.1925 \\ -1.0557 & -9.2672 \end{pmatrix}.$$

From this, we are able to calculate $trace = -9.2115495 < 0$ and $Det = 0.74308400 > 0$. So $(2.106, 12.555)$ is a stable node.
Another equilibrium solution $(2.904, 1.857)$ is tested similarly with a Jacobian matrix to calculate:

$$J = \begin{pmatrix} 0.0157 & 0.1279 \\ -1.0157 & -18.8479 \end{pmatrix}.$$

This matrix shows that the $trace = -18.83226319 < 0$ but $Det = -0.16524962 < 0$. These values fit the criteria of an unstable saddle, and show that $(2.904, 1.857)$ is unstable.

Figure 4.2 was generated by MATLAB ode45 (see Appendix). The solution curves in phase plane starting a sequence of initial conditions with initial predator varying from 0.1 to 10, and initial prey fixed at 2. It also shows the presence of Allee effects.

Example 3 (Allee Effects): Allee effects are also observed in the predators in Example 2. When the initial population in predators is less than 1.85, the corresponding solution will converge to extinct state. When the initial population in predators is greater than 1.87, the corresponding solution will converge to the coexistent state. See Figure 4.3.

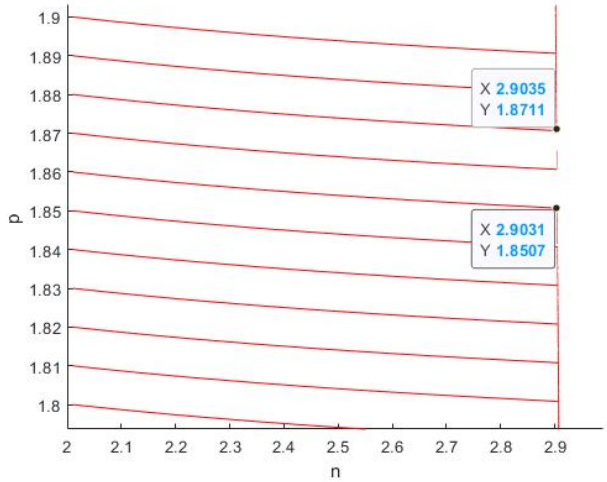

Figure 4.3: In the above figure, there is a small threshold between existence and extinction, an Allee effect, shown by the gap in the graphed line.

In the following graphs, we will numerically show the different phenomena that result when κ is varied.

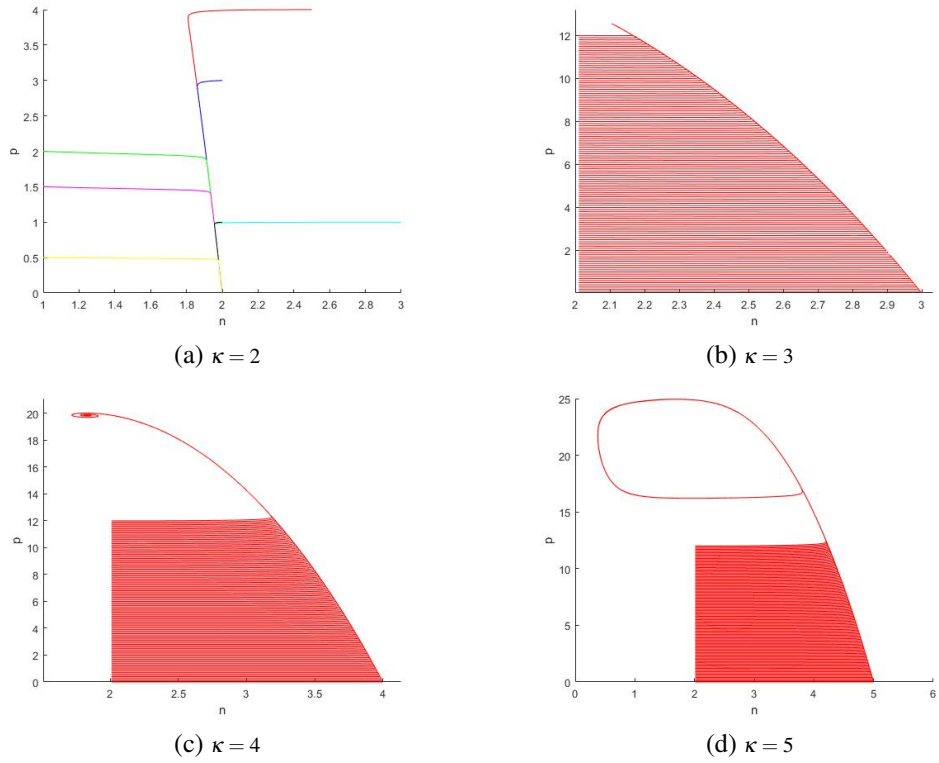

(a) $\kappa = 2$ (b) $\kappa = 3$

(c) $\kappa = 4$ (d) $\kappa = 5$

Figure 4.4: When κ varies from 2, 3, 4, and 5, the systems result in a stable extinct node (a), a stable coexistence node (b), stable spiral (c) and limit cycle (d), respectively.

In Figure 4.4, κ is no longer kept constant at 3, but the research is extended to values 2, 4 and 5. When κ is 2, there is no coexistent equilibrium solution, and the solution converges to $(\kappa, 0)$. In Figure 4.4 (a), solution curves starting from initial points $(1, 1.5), (3, 1), (1, 2)$ etc. are a few examples where solutions converge to $(\kappa, 0) = (2, 0)$. For the phase plane where $\kappa = 4$, a stable spiral appears. Stable nodes have a single trajectory to their equilibrium, but stable spirals will trace around their equilibrium in circles that get smaller and smaller until they reach their final stable, fixed point. Biologically, the population of the predator and prey are oscillating inward until they reach the point where the population of the predator and prey are constant. When $\kappa = 5$, again, a new phenomenon appears, a limit cycle. A limit cycle is a closed trajectory of a dynamical system. In this research, the stability of the limit cycle was not tested, but limit cycles can be stable, unstable, or both.

When plotting the prey and predator densities compared to the change in carrying capacity, κ, limit point and Hopf bifurcations become noticeable.

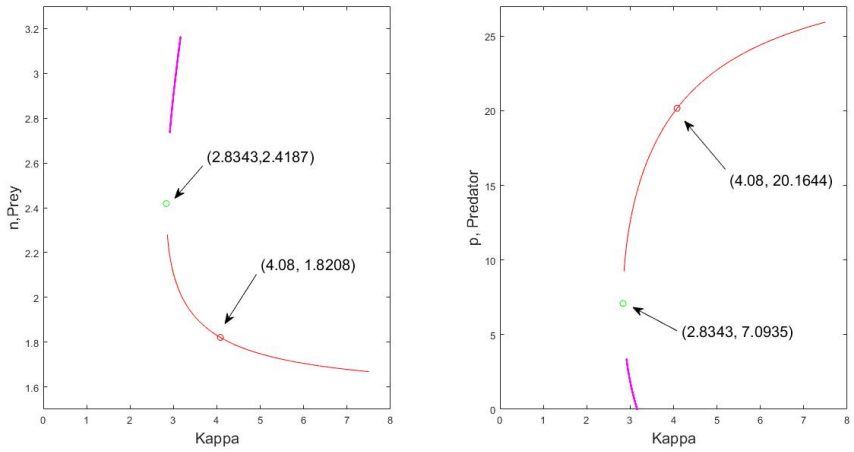

Figure 4.5: In the above diagram, $(2.8343, 2.4187)$ and $(2.8343, 7.0935)$ represent Hopf bifurcation, and $(4.08, 1.8208)$ and $(4.08, 20.1644)$ show the limit point bifurcations.

Figure 4.5 shows predator and prey graphed separately as κ is varied from 3 to 5. Where the stable node changes to a stable spiral, limit point bifurcation takes place which is represented by red circles in 4.5. As κ continues to increase to 5, Hopf bifurcation occurs. Hopf bifurcation takes place when a single stable point loses its stability, and a periodic solution originates. This occurs because the predator-prey relationship is transitioning from a stable spiral into a limit cycle. The Hopf bifurcation point is represented with a green circle.

MATLAB code, Bifurcations (see Appendix: Listing 6.3 Code Bifurcations), was used to produce this graph by calculating the stable and unstable points and plotting the predator and prey arrays separately as κ increases from 0 to 8.

Chapter 5

Conclusions

From our research, we were able to expand the Lotka-Volterra model using function response Holling type III. By using our newly derived model, we investigated the effects of varying the carrying capacity (κ). Our results showed three possible phenomena when κ took on the values of 3, 4, and 5. We observed a stable node, stable spiral, and limit cycle for each value of κ, respectively. Where κ was 3, a small threshold between existence and nonexistence, an Allee effect, was observed. Extinction in inevitable when the initial population in predators is less than 1.85, and coexistence takes place when the initial population in predators is greater than 1.87. Also, two types of bifurcation were noticed as κ increased, limit point bifurcation and Hopf bifurcation.

For our future research, we would like to discuss the behavior of the limit cycles, the basin of attractions for the stable equilibrium point, etc. Other possible future discoveries could come from varying other parameters while keeping κ fixed.

Chapter 6

Appendix

Listing 6.1: Code NullclineIntersections

```
clear all;

%establishing variables
sigma=20;kappa=3;alpha=.1 ;h_2=.9;

%setting the our models equations equal to x variables
n0=fzero(@(y) y*sigma*(1 - (y/kappa)) - (y^2 - 1 - h_2*y
   ^2) / (-alpha*y^2 + alpha*y^2 *h_2),5)
n1=fzero(@(y) y*sigma*(1 - (y/kappa)) - (y^2 - 1 - h_2*y
   ^2) / (-alpha*y^2 + alpha*y^2 *h_2),1)

n=0:0.000001:10;

%setting our nullclines equal to y variables
p1=n.*sigma .*(1 - (n./ kappa));
p2=(n.^2 - 1 - h_2.*n.^2) ./ (-alpha.*n.^2 + alpha.*n.^2 *
   h_2);

%plotting
figure
xlabel('n')
ylabel('p')
plot(n,p1,'b')
hold on
plot(n,p2,'m.')
hold on

%adds circles to the intersections of the nullclines
scatter([0 n0 n1 ],[0 (n0.*sigma.*(1 - (n0./ kappa))) (n1
   .*sigma.*(1 - (n1./ kappa))) ], 'ro')

axis on
axis([0 4.5 0 22])
```

The code NullclineIntersections was used to produce Figure 4.1. This code plots the two nullclines, and the intersections are circled for easier visibility. In order to produce Figure 4.1, all other parameters were kept constant while κ values were changed.

Listing 6.2: Code ode45

```
function [T,Y]=HuntingAllee2
%This is the Matlab code to solve differential equations.
   It consists two functions: one is the function which
   input the differential equations by providing the
   derivatives of the variables; one is the main function
   which implements the ODE45 to approximate solutions for
    IVP. dy/dx=F(x,y), y(x0)=y0.

for k=1:.5:10
%for k=10
%Use a single 'k' in order to produce a single solution
   curve
options = odeset('RelTol',1e-4,'AbsTol',[1e-6 1e-6]);
tend=100;
y0=[1,0.5]; %initial condition.
[T,Y] = ode45(@Holling3,[0 tend],y0,options);

%plotting
figure(2)
hold on
plot(Y(:,1),Y(:,2),'y')
xlabel('n')
ylabel('p')
end

function dy=Holling3(t,y)
%varaied kappa here to produce new phenomenas
kappa = 2; alpha = .1;  h2 = .9; sigma = 20;
n=y(1);p=y(2);
dy = zeros(2,1);    % a column vector
dy(1)=n * (sigma * (1 - n / kappa) - (alpha * p + 1) * n *
    p / (1 + h2 * (alpha * p + 1) * n ^ 2));
dy(2)=p * ((alpha * p + 1) * n ^ 2 / (1 + h2 * (alpha * p
   + 1) * n ^ 2) - 1);
```

Figures 4.2, 4.3, and 4.4 all were produced using a variation of Code ode45. This code will produce phase portraits and allows for phenomena to be displayed effectively.

Listing 6.3: Code Bifurcations

```
clear all

sigma=20; alpha=0.1; h_2=0.9;
p_stable=[];p_unstable=[];n_stable=[];n_unstable=[];

kappa_ini=2.8:0.0001:7.5;
for i=1:length(kappa_ini)
kappa=kappa_ini(i);
% Calculate the stable and unstable fixed points and save
   it into array p_stable,p_unstable,n_stable,n_unstable
   here.

    n1=fzero(@(y) y*sigma*(1 - (y/kappa)) - (y^2 - 1 - h_2
       *y^2) / (-alpha*y^2 + alpha*y^2 *h_2),5);
    n2=fzero(@(y) y*sigma*(1 - (y/kappa)) - (y^2 - 1 - h_2
       *y^2) / (-alpha*y^2 + alpha*y^2 *h_2),1);
    p1=n1.*sigma .*(1 - (n1./ kappa));
    p2=(n2.^2 - 1 - h_2.*n2.^2) ./ (-alpha.*n2.^2 + alpha
       .*n2.^2 *h_2);

    p_unstable=[p_unstable;p1];
    p_stable=[p_stable;p2];
    n_unstable=[n_unstable;n1];
    n_stable=[n_stable;n2];

end;

p_unstable_new = p_unstable(find(p_unstable > 0));
n_unstable_new = n_unstable(find(p_unstable > 0));

figure(1)
hold on
 subplot(1,2,1);
 % Plot kappa_ini vs n_stable,n_unstable here
 plot(kappa_ini(find(p_unstable > 0)),n_unstable_new,'m.',
    kappa_ini,n_stable,'r')
 hold on
 scatter([4.0800], [1.8208], 'ro')
 scatter([2.8343], [2.4187], 'go')

 axis([0 8 1.5 3.3])

 subplot(1,2,2);
```

```
% Plot p_stable,p_unstable vs kappa_ini here
plot(kappa_ini(find(p_unstable > 0)),p_unstable_new,'m.',
   kappa_ini,p_stable,'r')
hold on
scatter([4.0800], [20.1644], 'ro')
scatter([2.8343], [7.0935], 'go')

axis([0 8 0 27]);
```

Code Bifurcation was used to graph the predator and prey as κ increases from 0 to 8 in Figure 4.5. This code allowed the bifurcations to be shown easily by producing circles to pinpoint the locations at which they occurred.

Bibliography

[1] Courchamp F.; Berec L.; Gascoigne J.; 2010. Allee Effects in Ecology and Conservation. Journal of Mammalogy, 91, 1530–1532

[2] Stephens PA; Sutherland WJ; 1999. Consequences of the Allee effect for behaviour, ecology and conservation, Tredns Ecol Evol, 14,401–405

[3] Zhou, S.-R.; Liu, Y.-F.; Wang, G.; 2005. The stability of predator-prey systems subject to the Allee effects. Theor. Popul. Biol., 67, 23–31

[4] Wang, J.; Shi, J.; Wei, J.; 2011. Dynamics and pattern formation in a diffusive predator-prey system with strong Allee effect in prey. Journal of Differential Equations, 251, 1276-1305

[5] Wang, J.; Shi, J.; Wei, J.; 2011. Predator-prey system with strong Allee effect in prey. Journal of Mathematical Biology, 62, 291-331

[6] Rao, F; Kang, Y.; 2016. The complex dynamics of a diffusive prey-predator model with an Allee effect in prey. Ecological Complexity, 28, 123-144

[7] Avles, M; Hilker, F.; 2017. Hunting cooperation and Allee effects in predators. Jounral of Theoretical Biology, 419, 12-22

[8] Berec, L.; 2010. Impacts of foraging facilitation among predators on predator-prey dynamics. Bulletin of Mathematical Biology, 72, 94-121

[9] Xie, Z.; 2011. Turing instability in a coupled predator-prey model with different holling type functional responses. Discrete and Continuous Dynamical Systems Series, Volume 4, Number 6, 1621-1628

[10] Boukal, D. S.; Sabelis, M. W.; Berec, L.; 2007. How predator functional responses and Allee effects in prey affect the paradox of enrichment and population collapses. Theor. Popul. Biol., 72, 136–147

[11] Haile, D.; Xie, Z.; 2015. Long-time behavior and Turing instability induced by cross-diffusion in a three species food chain model with a Holling type-II functional response. Mathematical Biosciences, 267, 134-148